AGU PUBLICATIONS

JGR

Journal of Geophysical Research: Space Physics

RESEARCH ARTICLE

10.1002/2016JA023360

Postmidnight ionospheric troughs in summer at high latitudes

M. Voiculescu[1], T. Nygrén[2], A. T. Aikio[2], H. Vanhamäki[2,3], and V. Pierrard[4,5]

[1]Department of Chemistry, Physics and Environment, ECEE, Dunărea de Jos University of Galaţi, Galaţi, Romania, [2]Faculty of Sciences, University of Oulu, Oulu, Finland, [3]Finnish Meteorological Institute, Helsinki, Finland, [4]Royal Belgian Institute for Space Aeronomy, Space Physics and STCE, Brussels, Belgium, [5]Center for Space Radiations and Georges Lemaître Centre for Earth and Climate Research, Earth and Life Institute, Université Catholique de Louvain, Louvain-la-Neuve, Belgium

Key Points:
- The high-latitude plasma convection plays a role in formation and evolution of troughs in the postmidnight sector in sunlit plasma
- Ion temperatures are high at density minima (within the trough) at places where the convection plasma velocity is eastward and high
- A two-step process leads to formation of troughs in sunlit plasma: (1) energetic electron precipitation and (2) frictional heating

Correspondence to:
M. Voiculescu,
Mirela.Voiculescu@ugal.ro

Citation:
Voiculescu, M., T. Nygrén, A. T. Aikio, H. Vanhamäki, and V. Pierrard (2016), Postmidnight ionospheric troughs in summer at high latitudes, *J. Geophys. Res. Space Physics*, *121*, 12,171–12,185, doi:10.1002/2016JA023360.

Received 18 AUG 2016
Accepted 20 NOV 2016
Accepted article online 24 NOV 2016
Published online 22 DEC 2016

Abstract In this article we identify possible mechanisms for the formation of postmidnight ionospheric troughs during summer, in sunlit plasma. Four events were identified in measurements of European Incoherent Scatter and ESR radars during CP3 experiments, when the ionosphere was scanned in a meridional plan. The spatial and temporal variation of plasma density, ion, and electron temperatures were analyzed for each of the four events. Super Dual Auroral Radar Network plasma velocity measurements were added, when these were available. For all high-latitude troughs the ion temperatures are high at density minima (within the trough), at places where the convection plasma velocity is eastward and high. There is no significant change in electron temperature inside the trough, regardless of its temporal evolution. We find that troughs in sunlit plasma form in two steps: the trough starts to form when energetic electron precipitation leads to faster recombination in the *F* region, and it deepens when entering a region with high eastward flow, producing frictional heating and further depleting the plasma. The high-latitude plasma convection plays an important role in formation and evolution of troughs in the postmidnight sector in sunlit plasma. During one event a second trough is identified at midlatitudes, with different characteristics, which is most likely produced by a rapid subauroral ion drift in the premidnight sector.

1. Introduction

Ionospheric troughs are depletions in the *F* region density in the subauroral and auroral zone. According to the definition of *Rodger et al.* [1992], ionospheric troughs are regions at *F* region altitudes, typically a few degrees wide in latitude, where the plasma concentration is lower compared with regions immediately poleward and equatorward. Troughs known as *main troughs* or *midlatitude troughs* form generally in the premidnight sector, at relatively low (subauroral) geomagnetic latitudes of 55°–65° and are considered to be different types than *high-latitude troughs*. The latter forms inside and poleward of the auroral oval, usually not only on the dayside but also on the nightside in the postmidnight sector [*Rodger et al.*, 1992]. This distinction is more related to terminology, since studies based on large data sets have shown that there is no clear boundary, in space or time, between the two types of troughs [*Whalen*, 1989; *Horvath and Essex*, 2003; *Voiculescu et al.*, 2006; *Voiculescu and Nygrén*, 2007]. On the other hand, there are differences in the processes assumed to dominate in the formation of the trough at different times and latitudes. Troughs were originally considered to be phenomena occurring at night during winter [*Moffet and Quegan*, 1983; *Rodger et al.*, 1992]. More recent investigations, based on satellite records, have shown that troughs form during all seasons and also in day time, although the latter occur less frequently.

Various mechanisms for the generation of the trough have been suggested: increased recombination due to high temperatures or to more molecular composition, decreased production (due to lack of photoionization), or horizontal transport of different plasma of different densities. More than a single mechanism may contribute to trough formation, and their relative importance depends on geophysical conditions. A major mechanism of trough formation is enhanced recombination due to increased temperature. Electric field enhancements increase the ion temperature via ion-neutral frictional heating, which in turn accelerates the loss of positive ions via the reaction: $N_2 + O^+ = NO^+ + N$ [*Schunk et al.*, 1976]. The resulted molecular ion, NO^+, recombines much faster than O^+ and leads to rapid erosion of ionization. Another possible mechanism relates to the upward flow of plasma caused by heating and expansion associated with large relative ion-neutral drifts observed, e.g., in association with subauroral ion drifts (SAIDs) [*Anderson et al.*, 1991].

Table 1. Elevation Angles (Degrees) Used in the Latitudinal Scans With the UHF and ESR Radars[a]

UHF	20.0	24.0	28.6	34.7	43.6	55.0	70.0	90.0	103.0	116.0	125.6	138.0	146.0	152.0	156.6	160.3
ESR	34.0	42.0	50.0	58.0	66.0	74.0	82.0	90.0	98.0	106.0	114.0	122.0	130.0	138.0		

[a]The beam azimuth angle is 345° for both radars and elevation is calculated from the northward direction.

The ion-neutral frictional heating requires that there is a difference in ion and neutral velocities. During intense electric fields, the plasma velocities are typically much larger than neutral wind velocities, and wind acceleration at *F* region altitudes due to the ion drag is generally a rather slow process lasting order of hour to several hours [e.g., *Deng et al.*, 2009, and references therein].

A trough may form in the evening sector, near the equatorward edge of the dusk convection cell, when the plasma stagnates in darkness (i.e., when the westward convection flow within the dusk cell is balanced by the eastward corotation). The plasma decays due to lack of photoionization [*Whalen*, 1989; *Rodger et al.*, 1992; *Nilsson et al.*, 2005; *Voiculescu et al.*, 2010; *Spiro et al.*, 1978]. This cannot be the case for the postmidnight or morning trough, since most of the time convection is eastward. However, it may happen that the postmidnight trough is a continuation of the main trough [*Rodger et al.*, 1992]. Dayside troughs are observed in the afternoon sector and form most likely when the convection pattern has a particular configuration, which leads to replacing the photoionized plasma with decayed plasma transported across the polar cap from the nightside [*Pryse et al.*, 1998].

The statistical investigation of troughs made by *Werner and Prölss* [1997] shows that there are very few plasma depletions in the postmidnight sector, centered at about 70° geomagnetic latitude. In their statistical analysis of the *F* region depletion, *He et al.* [2011] have shown that during summer time there is a low chance that the trough forms at auroral magnetic latitudes. Using tomographic reconstructions of the ionosphere for 1 year (2003), *Voiculescu et al.* [2006] found that the number of troughs observed in summer is indeed lower compared to the other seasons. They found that troughs in summer are located mainly at high latitudes, around 68°–72°, are the narrowest of all seasons, and tend to stay at the same latitude. Consequently, most studies focus on troughs observed on the nightside, mostly in the premidnight sector. The high-latitude trough, which forms in the postmidnight sector, during summer, has got less attention. The results presented in the this paper aim at describing properties of this particular type of trough that may help in identifying trough formation in sunlight.

2. Experimental Data

2.1. Ionospheric Data

Experimental data come from the European Incoherent Scatter (EISCAT) radars. EISCAT is a scientific association operating incoherent scatter radar systems in northern Scandinavia. These aim at studying ionospheric and magnetospheric processes. In this work, we use the EISCAT UHF radars, located in Tromsoe (CGM: 66.6°N, 102.9°E), and the EISCAT Svalbard radar, ESR (75.4°N, 110.7°E) located near Longyearbyen.

Results from CP3 meridional scans of the EISCAT mainland and ESR radars were used for analyzing some properties of postmidnight troughs in summer in sunlit plasma. We consider summer extending from May to August. These experiments consist of latitudinal scans approximately in the geomagnetic meridional plane, with 16 (UHF) or 14 (ESR) positions, as listed in Table 1. One latitudinal scan takes 30 min. In the standard GUISDAP analysis [*Lehtinen and Huuskonen*, 1996] the number of range gates, the distance to the first gate, and the length of individual gates is varied with beam direction, so that all beam directions give data from the same height gates. There are 39 height gates between 77 and 574 km altitude for the UHF radar and 43 gates between 78 and 810 km altitude for the ESR radar.

The criteria of data selection were the following: (1) CP3 meridional scans experiments took place during summer (i.e., from May to August, when the postmidnight sector is mainly sunlit), and (2) the trough is observed during minimum three consecutive scans between 21:00 UT and 03:00 UT, roughly corresponding to 23:30–5:30 magnetic local times (MLT). A relatively low number of CP3 experiments during summer are available; thus, the number of events is also very small. Four troughs meeting the selection criteria were identified: three events observed during each night between 17 May 2004 and 20 May 2004, with both radars working, and one observed on 24–25 June 2003, when only the mainland radar was observing the ionosphere. The latter event is analyzed in detail in the companion paper [*Vanhamäki et al.*, 2016]. Four ionospheric

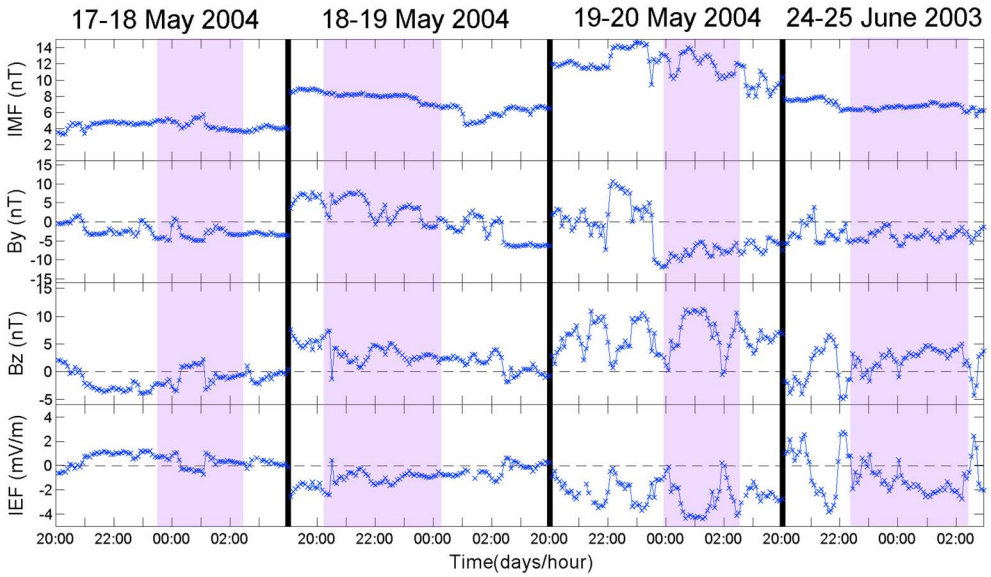

Figure 1. IMF data (total field, B_y, B_z, and E_y) in GSM coordinates, for the four night sectors (20:00 UT–04:00 UT) of 17–20 May 2004 and 24–25 June 2004, when troughs were observed. Each day/sector is delimited by solid, thick lines. Time intervals when the trough was observed are shown by superimposed colored rectangles.

parameters were analyzed: the electron density, the beam aligned ion velocity, and the ion and electron temperatures.

Tristatic measurements were also available, which allow calculating ion velocity vectors at the height of 300 km [*Nygrén et al.*, 2011]. However, the signal-to-noise ratio of the two remote receivers at Sodankyla and Kiruna were typically low; hence, ion velocities are available only during some short intervals (mostly during 24–25 June and, partially, during only one scan in 20 May). However, observations by Super Dual Auroral Radar Network (SuperDARN) radars allow examination of convection patterns [*Ruohoniemi and Greenwald*, 1996] including, at some particular times, information about the velocity at points within EISCAT field of view. Thus, if ion velocity measured by EISCAT cannot be calculated, convection patterns produced using SuperDARN tools were used for obtaining information about the plasma flow before and at moments when the trough is observed.

2.2. Global Conditions: Geomagnetic Activity and Interplanetary Magnetic Fields

Time series of 5 min interplanetary magnetic field (IMF) data and interplanetary electric field (IEF) data at the Earth's bow shock nose for the selected days were provided by the OMNIweb service (http://omniweb.gsfc.nasa.gov/). These are based on data from several satellites and are shown in Figure 1. Geomagnetic activity was low during all events, with K_p between 0 and 2. Figure 1 shows that the IMF is relatively stable during most scans, implying that the convection is relatively stable during trough observations. Time intervals when troughs are observed are marked by colored areas. The IMF B_z is northward (positive) for three troughs, meaning that the convection pattern is confined to high latitudes. The IEF is mostly negative during all events, which supports the assumption that the ionosphere is relatively quiet. Rapid variations of both B_y and B_z components are observed during 19–20 May 2004, which most likely disrupt convection patterns, affecting the formation and evolution of the trough. *Voiculescu et al.* [2006] found that very few troughs are observed during high geomagnetic activity in the postmidnight sector. They also have shown that during quiet times, troughs may be seen after midnight mostly for positive B_z and negative B_y. This distribution was explained by *Voiculescu and Nygrén* [2007] taking into account the convection pattern dependence on IMF structure and the possible impact on trough formation.

3. Results

Figures 2, 4, 6, and 8 show the temporal and spatial evolution of the ionospheric parameters for each of the four cases: plasma density at 320 km and at 120 km and electron and ion temperatures at 320 km. The density in the *E* region shows whether signs of particle precipitation exist before or during the trough occurrence.

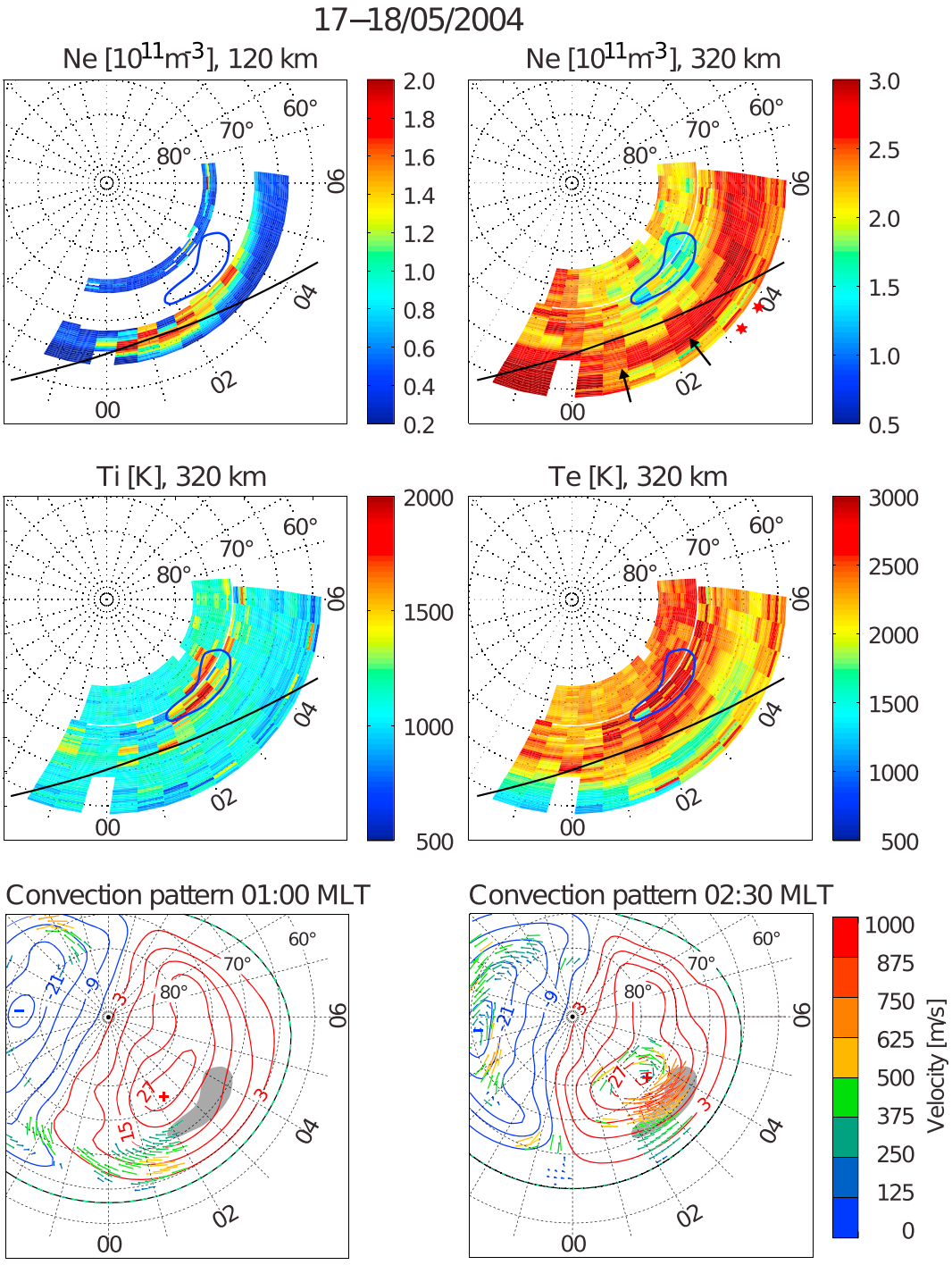

Figure 2. Variation of ionospheric parameters measured by EISCAT, in geomagnetic coordinates, during the night of 17–18 May 2004. Plasma density (N_e) at 120 km and 320 km (top row), ion (T_i) and electron (T_e) temperatures at 320 km (middle row), and convection patterns at two different UT times (bottom row); the corresponding MLT are indicated by arrows in the top right plot. The average position of the high-latitude trough is shown as a grey area. The solar terminator is shown as a black line. Red stars indicate the MLT corresponding to the start of individual scans shown in the next figure.

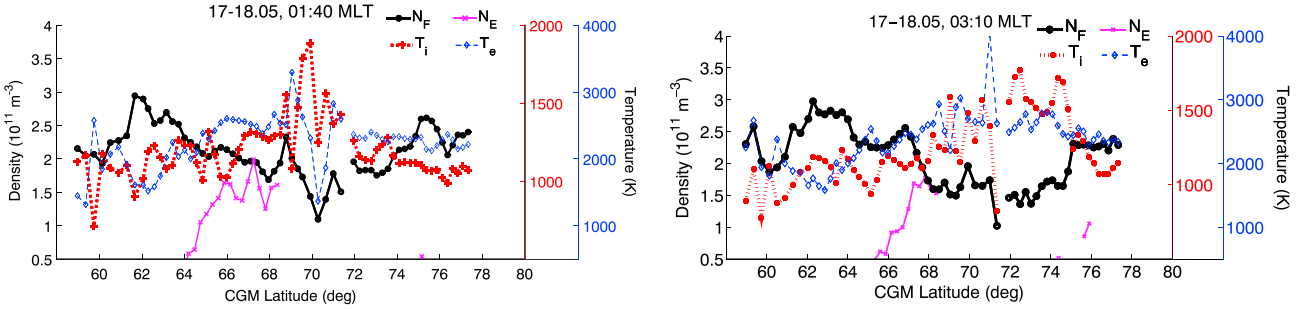

Figure 3. Horizontal variation of ionospheric parameters for two selected meridional scans during 17–18 May 2004. The black (magenta) line shows electron density at 320 km (120 km). Ion temperature is marked by a red line, and electron temperature is shown in blue. Only densities higher than $0.5 \cdot 10^{1}1$ m^{-3} are shown in the plot.

Because the meridional scan of the radar covers a smaller latitudinal range in the *E* region, there is a gap in the spatial variation of Ne at 120 km between ESR and EISCAT mainland data. The same height is used for all four events to allow the comparison between the environmental conditions between the four events. The troughs are presented in magnetic coordinate system (magnetic latitude (MLAT), MLT). The troughs are not steady structures, and they are evolving in a Sun-fixed frame, since they are viewed sequentially by a radar that rotates beneath the *F* region. Thus, the following figures do not represent instantaneous pictures of the whole region; however, since the ionosphere is relatively quiet, one can assume that the radar gives a reliable image of the trough evolution.

Convection patterns for selected time instants during the period of trough observation, generated by the SuperDARN model [*Ruohoniemi and Greenwald*, 1996] are displayed in the bottom row of each figure. For most nights, plasma velocity measurements from SuperDARN radars were available, and they are also shown in the convection plots. The approximate location of the trough center is shown in these plots using a grey area, in order to identify the role played by convection in trough formation. Each polar plot is followed by examples of the horizontal variation of the ionospheric parameters during selected scans, i.e., Figures 3, 5, 7, and 9.

When studying the SuperDARN convection patterns, it should be remembered that in areas where there are no data, a statistical background model is used [*Ruohoniemi and Baker*, 1998]. In some cases, like Figure 2 at 02:30 MLT, there are good data on the trough area, so the convection pattern there should be reliable. However, even in the case of Figure 2, the large-scale convection pattern (e.g., in the polar cap and dayside) may be uncertain due to lack of global data coverage. We can of course think that when there is no data, the SuperDARN convection map is our best guess for the large-scale convection based on statistical correlations with solar wind parameters. However, even if statistically correct, it may not be very representative for single events. Thus, the SuperDARN convection maps shown in Figures 2, 4, 6, and 8 should be considered as sketches of the most likely situation.

3.1. Trough 17–18 May 2004

During the night of 17–18 May 2004, the trough is observed between 01:00 and 04:00 MLT and is centered at about 70° Geomagnetic Latitudes (Figure 2). Densities inside the trough reach minima of about $1.5 \cdot 10^{11}$ m^{-3}. The plasma density at earlier times and equatorward of the trough is more than $3 \cdot 10^{11}$ m^{-3}, but the poleward wall is shallower. The ion temperature is 1000–1500 K in the whole area, except in the trough, where it reaches 2500 K or more. A relatively small increase of electron temperature T_e is observed poleward of the trough. Figure 3 shows that the trough is relatively wide and not very deep and walls are shallow. High density in the *E* region is seen in the southern part of the trough as long as the *E* region is seen by the radar.

The southward IMF B_z produces a two-cell convection pattern which persists during the entire time of trough observation. Eastward velocities in the postmidnight sector reach 800–1000 m/s in the region of trough minimum between 02:00 and 04:00 MLT. Note that regions of high plasma density in the *F* region (top right plot) match the external convection lines of the dawn cell.

3.2. Trough 18–19 May 2004

The deepest trough is observed during 18–19 May 2004 between 23:00 and 03:00 MLT (Figures 4 and 5).The trough is well defined, latitudinally elongated, very narrow (1–2°), and relatively deep. Minima of $1.5 \cdot 10^{11}$ m^{-3} are observed around 69°–70° MLAT. A thin strip of relatively modest increase of *E* region density is observed

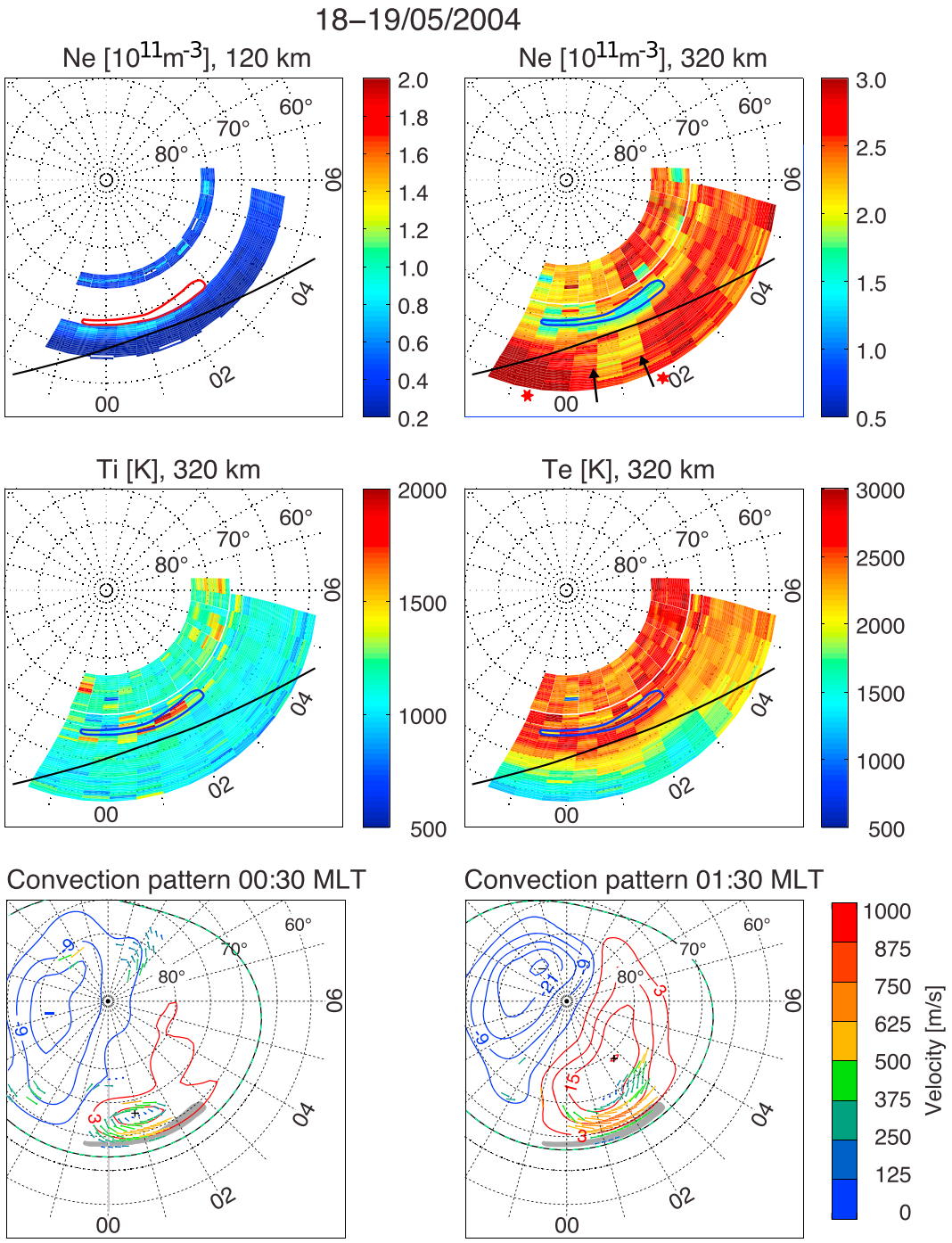

Figure 4. Variation of ionospheric parameters in geomagnetic coordinates during the night of 18–19 May 2004. Similar to Figure 2.

at the southward border of the trough. Increases in the ion temperature are observed inside the trough, at a smaller scale than in the previous case. The electron temperature in the trough region is similar to the previous night, with values of 2500–3000 K that extend poleward of the trough, in the illuminated area. T_e has low values (1500–1800 K) equatorward of the trough, close to the terminator, and no clear variation inside the trough. Figure 5 shows that T_i increases occur at the minimum and at the poleward wall of the trough.

The SuperDARN measurements show that the flow is strongly eastward inside the trough, around 70°, where the trough minimum is located. Later at some point the convection cells shrink, according to the SuperDARN

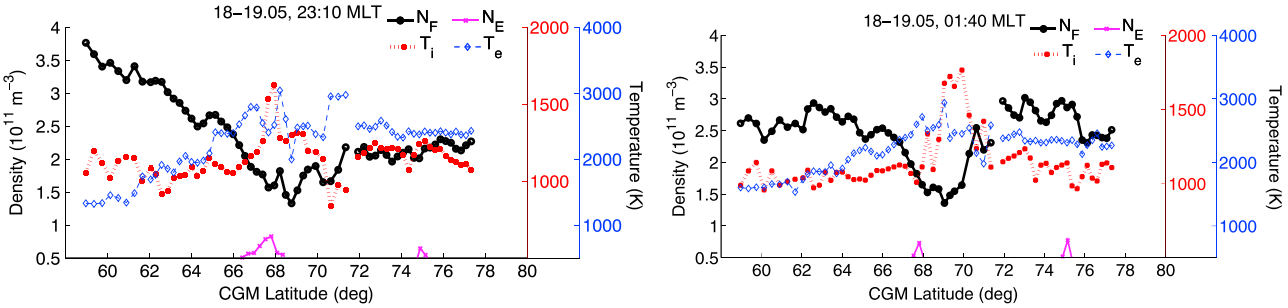

Figure 5. Horizontal variation of ionospheric parameters for two selected meridional scans during 18–19 May 2004. Similar to Figure 3.

convection patterns, which is typical for northward IMF conditions. The trough slightly moves outside of the dawn cell, where the ion velocity is rather small and where the ionization builds up fast due to photoionization. Relatively high ion velocities (700 m/s) are measured by SuperDARN radars in the area of the trough minimum.

3.3. Troughs 19–20 May 2004

On 19–20 May 2004 a localized deep structure is observed between 65° and 75° MLAT between 3:00 and 5:00 MLT (Figure 6). Figure 7 shows that the trough has minima less than 10^{11}m^{-3} centered at 66.5°, with sharp walls around 3:00 MLT. The ion temperature is high inside the trough. Some increases of the electron temperature are observed locally. The trough seen on 19-20 May forms in an already depleted ionosphere, whose ion temperature is, locally, relatively high. Some precipitation exists in the E region, in the southern part of the trough.

The convection pattern on this night has initially two weak cells with some plasma flow increase at times when the trough is observed. Although no information about ion velocities exists for the trough area, it is interesting to note that the trough on 19-20 May 2004 disappears at the point where the modeled plasma convection turns poleward and that the shape of the trough nicely follows the convection lines at the outer edge of the dawn convection cell.

On this particular night another trough is observed at the equatorward edge of the radar field of view, with a minimum plasma density at 60° CGMLAT. The trough is narrow (max 2°) and lasts for the entire observation interval, although around 02:00 MLT both walls start to fade. This is a trough whose properties (and thus formation mechanism) is different from the high-latitude troughs considered for the present study: the trough can be considered as a mid-latitude one, the electron temperature abruptly increases within the trough and a relative ion temperature increase is locally seen. The trough is located outside the convection cells, where only the corotation governs the plasma flow.

3.4. Trough 24–25 June 2003

The fourth event has a poorer coverage, since the observation starts later, at 00:30 MLT and no ESR observations are available to observe higher latitudes (Figures 8 and 9). The trough is seen between 65° and 70° MLAT from 01:00 MLT to 06:00 MLT. It is not clear whether at 6:00 MLT the trough fills in (i.e., disappears) or retreats to higher latitudes, where no radar coverage exists. No poleward wall is seen, but this may be due to the fact that the radar field of view reaches the maximum of 72° MLAT. Observations during the last two scans, between 05:00 and 06:00 MLT, suggest that the trough fills in because there is no clear poleward movement of the minimum density. Some characteristics are partly similar to those of the first trough: high ion temperatures coincide with maximum density decreases, there is some minor variations of the electron temperature, and energetic *E* region precipitation is observed equatorward of the trough. This event is analyzed in detail in *Vanhamäki et al.* [2016].

There are no SuperDARN radar measurements of plasma velocity at the moment of trough observation. According to SuperDARN statistical model, the trough is located on the equatorward side of the dawn cell in areas where the eastward flow is not high.

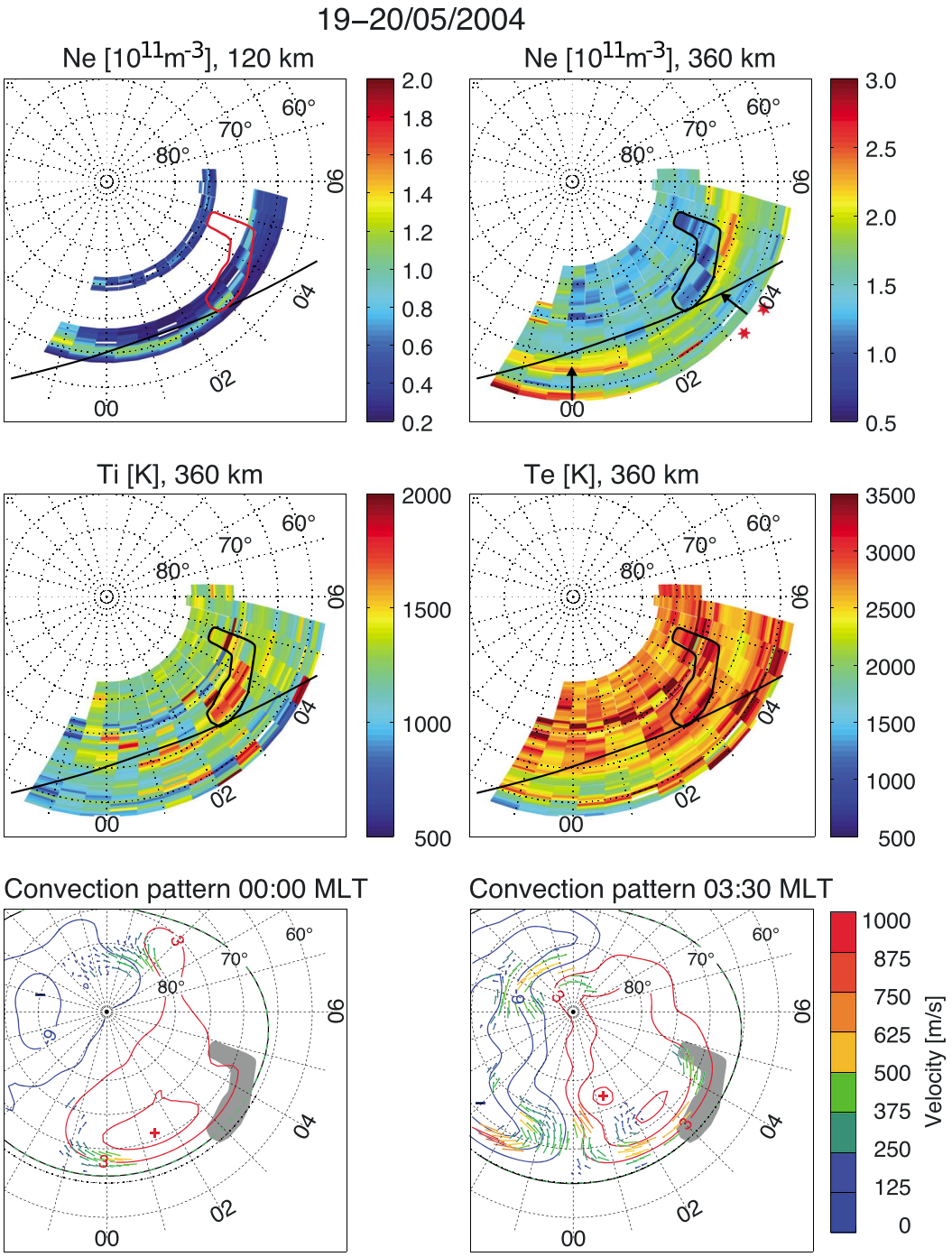

Figure 6. Variation of ionospheric parameters in geomagnetic coordinates during the night of 19–20 May 2004. Similar to Figure 2.

4. Discussion

All high-latitude troughs described in section 3 display some common features:

1. The troughs are observed in sunlit plasma (which was the main selection criterion) in the postmidnight sector, between approximately 02:00 and 04:00 MLT, around 70° MLAT.
2. The troughs are not very deep, and their walls are generally shallow.
3. Increases of the plasma density in the *E* region, close to the equatorward edge of the trough, are observed, suggesting that particle precipitation might play a role in the evolution of the trough.

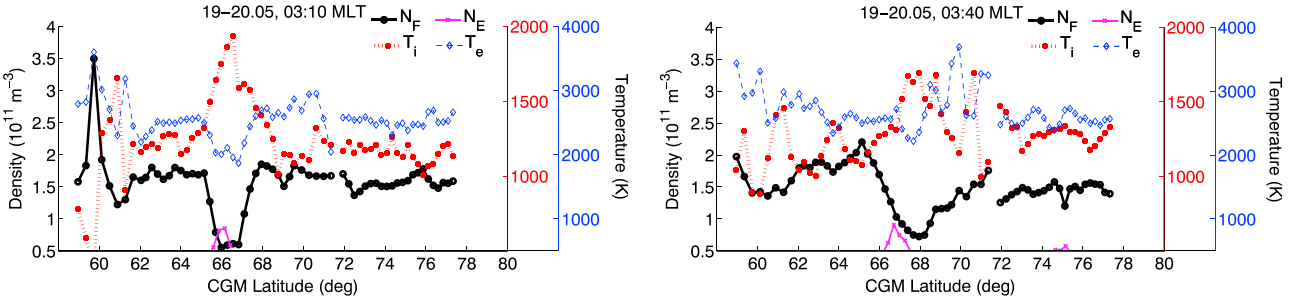

Figure 7. Horizontal variation of ionospheric parameters for two selected meridional scans during 19–20 May 2004. Similar to Figure 3.

4. The ion temperature is high inside the trough, where the plasma depletion is maximum.
5. Small increases in the electron temperature are observed sometimes in the trough; however, these extend over large areas and for long time; thus, the association with the trough is not clear.
6. For the three troughs in May the plasma flow is eastward, as shown by SuperDARN radar measurements; for two of them (17–18 and 18–19 May) the flow speed is high, with high ion velocities in areas where troughs are observed. For the trough in 24–25 June 2003, analyzed in detail by *Vanhamäki et al.* [2016], the flow is also eastward. At moments when there are no measurements colocated with the trough, the modeled pattern suggests that the flow remains eastward.

The high-latitude trough on 18–19 May 2004 stands out: it is sharp, narrow, deep, and is well defined. It forms earlier than the other troughs and lasts for a longer time. The *E* region density and precipitation are weakest during this event. One could say that this is an example of a "clean" trough, given the lack of energetic precipitation within the trough area, i.e., a trough whose formation is most likely due to one process only.

Obviously, it is not clear whether the troughs are steady structures or constantly evolving in a Sun-fixed frame, since they are viewed sequentially by a radar that rotates beneath the *F* region. However, one can safely assume that the plasma is depleted by a mechanism that acts on a continuous basis and produces a trough that is visible during some time in different locations. One mechanism for trough formation in the premidnight sector, confirmed by numerous studies, is the stagnation mechanism: eastward corotation cancels the westward convection, plasma stagnates in the nonilluminated areas, and its density drops due to lack of solar (UV) ionization [*Rodger et al.*, 1992; *Nilsson et al.*, 2005; *Voiculescu et al.*, 2010; *Voiculescu and Nygrén*, 2007]. Since the position of all four troughs is related to the dawn convection cell, one can assume that plasma convection may contribute to the formation and evolution of postmidnight troughs as well. However, the mechanism itself is different from premidnight or winter troughs, where the main assumption is that plasma density decreases due to stagnation in darkness. High-latitude summer troughs in the postmidnight sector are located almost entirely in sunlight. Moreover, both corotation and convective transport are eastward; thus, stagnation is not possible. A trough may form in sunlit regions when, e.g., low-density plasma convects from the nightside to the dayside, replacing the high-density plasma [*Whalen*, 1989; *Rodger et al.*, 1992; *Pryse et al.*, 1998; *Mallis and A Essex*, 1993]. This mechanism acts on the dayside and can be rejected for these particular summer troughs, since the regions where the troughs form are continuously fed with high-density plasma brought by the antisunward convection from the noon sector.

A third mechanism relates to plasma density decreases produced by increased recombination following frictional heating, which in turn is due to high ion velocities. *Vanhamäki et al.* [2016] have shown that the electron density in areas of large plasma flow can be reduced by approximately a quarter, compared to the surrounding environment. Heating may also lead to upwelling of the neutral atmosphere, making the ionosphere more molecular, which leads to faster recombination. The ion temperature is high in all troughs, which indicates that the latter mechanism is most likely at least one reason for plasma depletion. Moreover, the ion temperature is highest at the trough minima. The reason for ion temperature increase cannot be readily associated with high ion velocities in all cases because measurements of ion velocities are not reliable for all four events. However, all convection patterns look rather similar at times when the trough is observed: they have two cells which, at the moment of trough formation, are pretty well defined. Also the deepest regions are colocated with large eastward ion velocities (more than 600 m/s in the Earth fixed frame), for at least three of the four cases (Figures 2, 4, and 8). For the other event (Figure 6) some indications of high ion flow exist, at least in the beginning of trough formation. All troughs disappear while progressively exiting regions of convection.

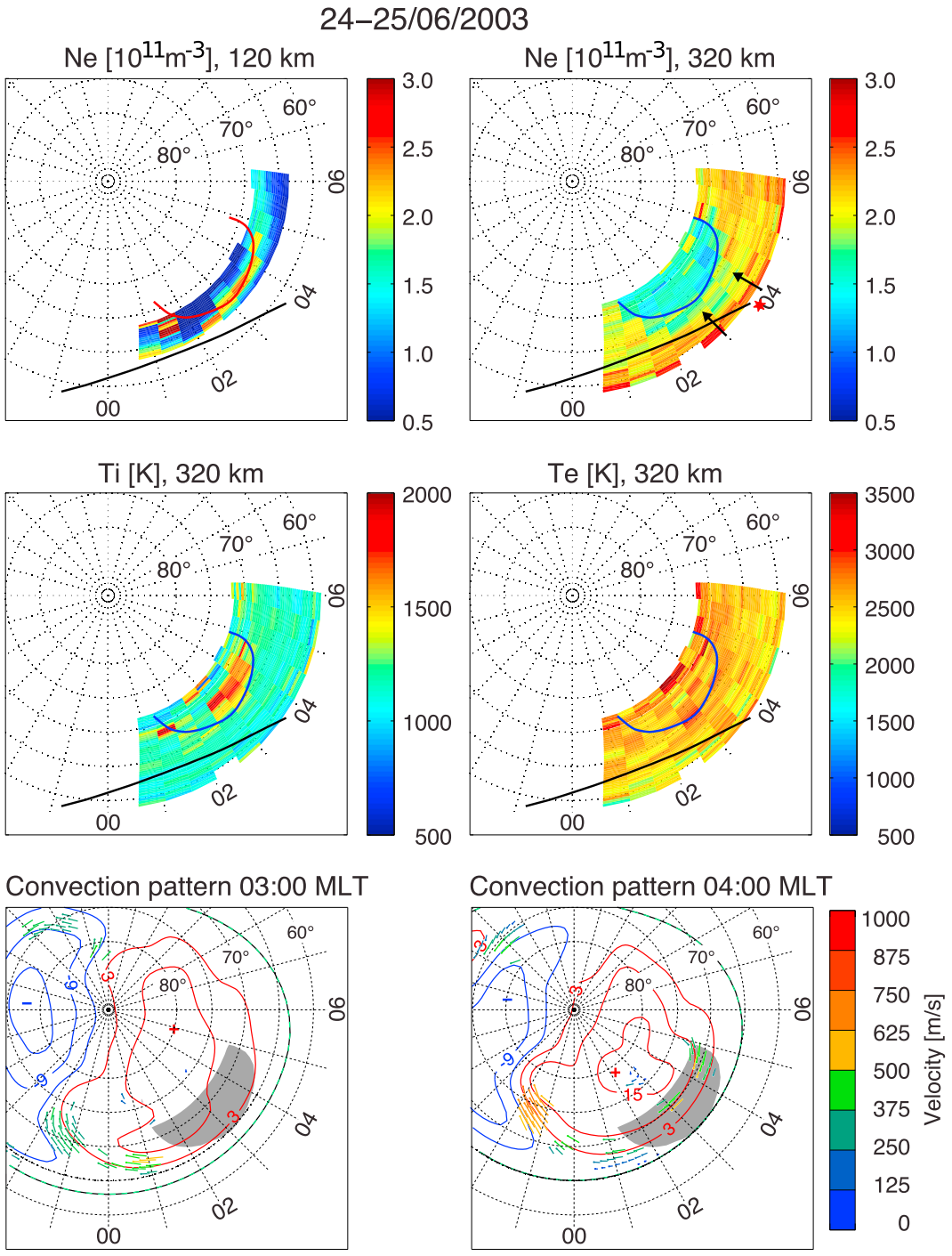

Figure 8. Variation of ionospheric parameters in geomagnetic coordinates during the night of 24–25 June 2003. Similar to Figure 2.

Eastward convection adds to corotation velocity, increasing the ion speed in the Sun-fixed frame reference. The nicest example supporting the role played by the convection pattern on trough formation at high latitudes is seen in Figure 6, where the trough seems to end at a kink in the convection pattern.

Zou et al. [2013] have shown that trough formation at morning, at high latitudes, might be connected to upward electron flux associated with downward field-aligned current (FAC). This is supported also by simulations of *Nilsson et al.* [2005] for evening troughs which show that such a process results in increasing the ion loss rate and plasma density erosion. *Vanhamäki et al.* [2016] observe that for the trough on 24–25 June 2003,

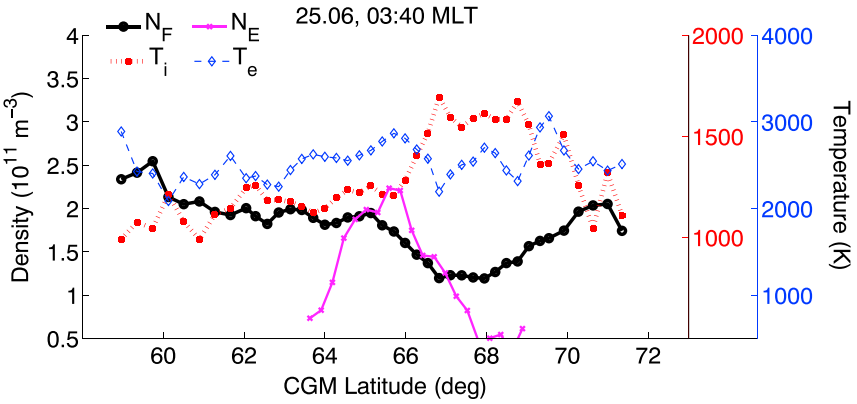

Figure 9. Horizontal variation of ionospheric parameters for a selected meridional scan during 24–25 June 2003. Similar to Figure 3.

vertical currents are upward at the poleward side and downward in the center, where the density has the minimum, as well as on the equatorward side, which may contribute to shaping the trough. They suggest that downward FAC may create initially a small ionospheric depletion, which further develops into a trough when entering a region with large eastward plasma flows leading to ion heating.

Convection maps at moments of trough observation suggest that convection might play an important role in shaping the *F* region plasma density in the postmidnight sector at high latitudes. Indeed, the shape of the convection pattern is based on a statistical model, even if in some cases there is a good coverage in the trough area. The large-scale convection pattern may be uncertain (e.g., in the polar cap and on dayside) due to lack of global data coverage. In the absence of data, however, the modeled convection is a best guess for the large-scale convection based on statistical correlations with solar wind parameters and existing measurements. The depleted ionosphere on 19–20 May 2004 (Figure 6) is likely the result of the particular shape of convection cell during the first hours of the night. Before 02:00 UT (04:30 MLT) the pattern is heavily distorted, with a small dawn cell located at relatively low latitudes. This forces plasma to convect within a region close to solar terminator, with a large solar zenith angle and a relatively low level of solar ionization. As the plasma density gradually decays, the *F* region becomes more neutral and molecular [*David et al.*, 2002] which could be the reason for the low electron density.

The other three high-latitude troughs (17–18 and 18–19 May 2004 and 24–25 June 2003) form in regions where the plasma density is high (Figures 2, 4, and 8). The walls are more abrupt and the trough is better defined. In these cases the morning convection is well defined, favoring that the *F* region is continuously fed by high-density plasma from the dayside near the solar terminator.

The differences between wall densities are not significant. The equatorward walls have, most of the time, higher density (sometimes reaching $3.5 \cdot 10^{11}$ m^{-3}) than poleward walls (roughly $2-2.5 \cdot 10^{11}$ m^{-3}). Signatures of precipitation at the equatorward side are seen at lower altitudes. This, combined with the distribution of electron temperature, indicates that the equatorward wall may be part of the auroral oval, while the poleward wall is made of dayside *F* region plasma carried from the dayside. However, this is not necessarily true for the entire period of trough development (e.g., Figures 6 and 8).

A relative increase of T_e can also be seen, but this is due to decreasing of solar zenith angle [e.g., *Schunk and Nagy*, 1978]. Thus, no clear association with increased electron temperature can be made. The behavior of T_e in these troughs is different compared to the premidnight trough, where the electron temperature is usually high [e.g., *Rodger et al.*, 1992; *Pryse et al.*, 1998; *Voiculescu et al.*, 2010]. Some isolated peaks of the electron temperature can also be spotted, but these are local and sporadic. These may be the consequence of dissociative recombination triggered by heated ions in the trough [*Schunk and Nagy*, 1978], since signatures of large electric fields that may also increase the electron temperature do not exist.

The high ion temperatures coinciding with trough minima, in all cases, suggest that the plasma is depleted due to ion heating, when plasma drifts at large speed relative to neutrals. Heating leads to accelerated recombination and rapid plasma depletion. The mechanism of postmidnight troughs observed in summer relies on ion heating effects on surrounding plasma in the illuminated *F* region, which are associated to large

Table 2. Position of Plasmapause at Different MLT

Trough	MLT	MLAT	MLT	MLAT
17–18.05.2004	01:00	62.21°	02:30	60.79°
18–19.05.2004	00:30	61.53°	01:30	61.17°
19–20.05.2004	00:00	61.53°	03:30	60.40°
24–25.06.2003	03:00	60.00°	04:00	59.58°

zonal velocities generated by magnetospheric electric fields. Energetic precipitation, suggested by increased *E* region density, is seen on the equatorward side of most troughs. Some exception is seen for the trough on 19–20 May 2004 (Figures 6 and 7) for which the *E* region density enhancement is located closer to the trough minimum. The precipitation lies northward of the solar terminator, usually in sunlit plasma. Photoionization and energetic precipitation may deposit sufficient energy to trigger the upward flow [*Redmon et al.*, 2012; *Anderson et al.*, 1991], bringing more molecular plasma to *F* region heights, thus accelerating recombination and reducing plasma density. Initially, when there is no heating, the trough is shallow. An important mechanism is the fast recombination of NO^+, following a more efficient production of this molecular species, which is highly dependent on temperature [*Schunk et al.*, 1976]. *Vlasov and Kelley* [2003] have shown that deep troughs, observed during storms, could be created by vibrationally excited N_2 following energetic precipitation. Recombination due to this type of molecular species (including also O_2) could cause a 30% depletion in plasma density, according to, e.g., *Pavlov and Foster* [2001]. Hence, plasma depletion caused by increasing density of excited molecular species should also be considered as a possible cause for the trough.

Thus, the formation of summer postmidnight troughs could be due to a two-step mechanism. First, molecular species get vibrationally excited due to precipitation, starting to reduce the plasma density. Next, the increasing eastward ion velocity heats the ions, which recombine faster and deepen the existing shallow trough.

One parameter that should be considered in identifying trough formation mechanisms is the neutral wind [*Vlasov and Kelley*, 2003]. Models of neutral winds [*Deng and Ridley*, 2006; *Förster et al.*, 2008] show that, in the postmidnight sector of the Northern Hemisphere, the neutral wind is generally antisunward and eastward. Such a wind lifts the plasma up, bringing more molecular ions to *F* region altitudes and speeds up the recombination. In the postmidnight sector, where the convection is mostly eastward, the *F* region plasma convection and the neutral wind make an angle. The differential motion may heat the ions, as long as neutral does not respond to ion drag. The latter effect is relatively slow; however, it may be possible that the decay of the ion temperature at later stages of the trough may be due also to neutrals catching up ions. Thus, winds may play an important role in the evolution of the trough in the postmidnight sector.

4.1. Postmidnight Trough at Midlatitudes

The midlatitude trough observed at magnetic latitudes of 60°–61°, around magnetic midnight (*trough L*), is of a different type (Figures 6 and 7). This trough has most likely formed previously in the premidnight sector. The characteristics of this particular trough are different, compared to the high-latitude troughs: the electron temperature is high inside the trough and relatively low on walls, while the ion temperature does not vary significantly. The trough is narrow, with relatively steep walls. Information about the *E* region density is not available (due to radar geometry). This particular latitude is usually associated with the plasmapause. The location of plasmapause for all four events is given in Table 2 for comparison.

The plasmapause location is determined from the model developed by *Pierrard and Cabrera* [2005], where the geomagnetic activity level during the previous 24 h determines the convection and thus the position of the plasmapause by interchange instability. The model is MLT dependent and shows excellent agreement with plasmapause observations of IMAGE, Cluster, and CRRES [*Pierrard and Cabrera*, 2005; *Verbanac G. et al.*, 2015; *Bandic et al.*, 2016].

High electron temperatures may be considered as a possible signature of plasmapause in the ionosphere [*Pierrard and Voiculescu*, 2011]. During 17–18 May 2004 the *F* region plasma is depleted at about 61°, which is close to the plasmapause location in Table 1. The electron temperature is high at the same latitude, which suggests that the shallow depletion at low latitude may be considered as the plasmapause signature. However, since no other mechanism is at play, there is no further development into a midlatitude trough. No similar depletion exists at lower latitudes during 18–19 May and 24–25 June in the postmidnight sector.

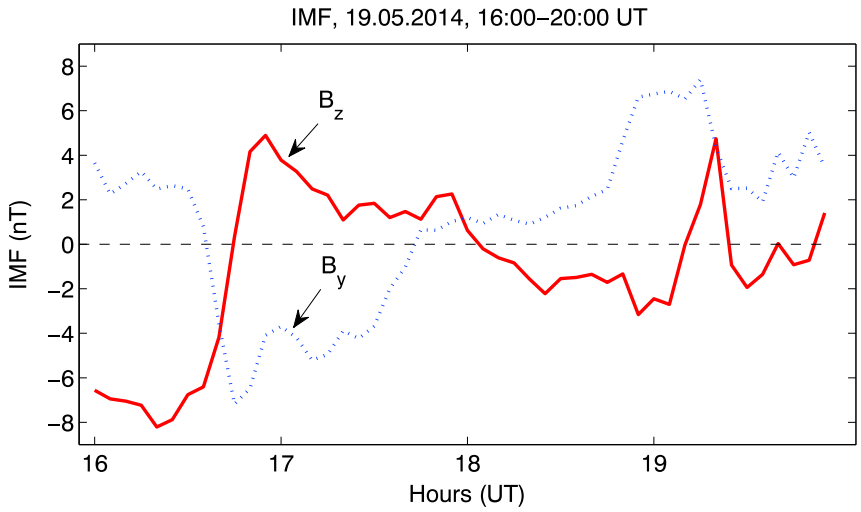

Figure 10. IMF variation before trough L was observed.

On 19–20 May 2004 the location of trough L, observed at midlatitudes corresponds to the plasmapause location. The trough is deep, elongated, and lasts for several hours. Since the trough formed sometimes before radar measurements started, we investigated the premidnight conditions on 19–20 May 2004. A_p and K_p indices increase between 12:00 and 18:00 UT. Figure 10 shows that B_z was southward and large until 16:50 UT (19:20 MLT), when it abruptly turned to northward. Such reversals produce usually overshielding, i.e., the dawn-dusk convection electric field becomes suddenly smaller than the shielding electric field, assumed to be linked to region 2 FAC [*Ebihara et al.*, 2008]. These in turn are considered to be possible causes for subauroral ion drifts (SAIDs) [*Anderson et al.*, 2001; *Voiculescu and Roth*, 2008]. SAIDs occur mostly during the recovery phase of a substorm [*Anderson et al.*, 2001]. According to the *AE* index, such a substorm took place shortly before the trough started to be observed (not shown). SAIDs are most of the time associated with premidnight troughs [*Anderson et al.*, 2001; *Voiculescu and Roth*, 2008, and references therein]. The DMSP F15 satellite measurements (not shown here) show that a peak exists in the westward ion velocity, of approx 700 m/s, at about 61–62° at 18:00 UT (20:40 MLT). Both T_i and T_e at DMSP altitudes are high, and high plasma temperatures are observed in association with SAIDs [*Anderson et al.*, 2001; *Voiculescu and Roth*, 2008]. Thus, one can assume that trough L is a structure that formed earlier possibly as a consequence of a SAID. After the rapid shrink of the convection pattern, following the B_z turn, the structure detached from the convected plasma and corotated, entering the postmidnight sector.

The high electron temperature in trough L could be caused by dissociative recombination, deactivation of excited species, collisions with heated ions/neutrals, heat conservation along the flux tube, or energy deposition by precipitation [*Schunk and Nagy*, 1978, and references within]. Dissociative recombination results in heating of the electron ensemble, since cold electrons recombine faster than hot electrons; thus, on the average, there are more hot electrons left to contribute to increasing electron temperature. *Schunk and Nagy* [1978] have shown that at plasmapause heating is transported along magnetic field lines to the ionosphere, resulting in regions with elevated electron temperature. Considering the location of trough L and the fact that the main trough is associated to plasmapause [*Pierrard and Voiculescu*, 2011], this seems to be the most probable explanation. *Anderson et al.* [2008] showed that the ionospheric projection of the plasmapause is associated with the H^+ trough. The subauroral elevated electron temperatures have been associated also with stable auroral red arcs. The latter may be considered as indicating the location of the plasmapause during the main and recovery phase of a geomagnetic storm [*Mendillo et al.*, 2013]. Taking into account the coincidence with the modeled location of the plasmapause, one could speculate that trough L may be considered as a possible plasmapause signature.

5. Conclusions

Measurements of EISCAT incoherent scatter radars were used for investigating some properties and the formation mechanisms of the postmidnight ionospheric trough during summer in the illuminated plasma.

Observations of SuperDARN radars including plasma velocity measurements within EISCAT field-of-view and associated model convection patterns [*Ruohoniemi and Greenwald*, 1996] were used for plasma flow information.

Four events were identified, the small number being due to the scarcity of summer EISCAT CP3 measurements. Postmidnight troughs form in summer at magnetic latitudes centered at 70°, are accompanied by high ion temperatures and no (or small) electron temperature variations, and have relatively small wall density gradients. Ion velocities and ion temperatures are high at locations of trough minima. Their width may vary from 2° to 5° or more. Precipitation at the equatorward part of the trough (inside or close to the wall) is seen during most events, with various intensities. In one case there is almost no increase in the *E* region densities at trough latitude; in this case the trough is narrow, well structured, and forms at earlier magnetic local times. These high-latitude troughs are all colocated with eastward flow within the dawn cell such that the trough vanishes/fills in when going out of the cell.

The most probable mechanism of trough formation seems to be a two-step one: the trough starts to form when energetic electron precipitation leads to faster recombination in the *F* region due to upward motion of molecular ions, followed by plasma depletion, and it deepens when entering a region with high eastward flow, producing frictional heating and further depleting the plasma. Thus, convection plays an important role in formation of the postmidnight sector, although the formation mechanism is not stagnation, as in the premidnight sector, but frictional heating associated with large eastward velocities.

A second type of trough was observed at midlatitudes during one night, with properties that are different from those of the high-latitude trough. This particular trough, which coincides with plasmapause location, is most likely produced in the premidnight sector by a SAID.

Acknowledgments
EISCAT is an international association supported by China (CRIRP), Finland (SA), Japan (STEL and NIPR), Germany (DFG), Norway (NFR), Sweden (VR), and United Kingdom (STFC). The work of M.Voiculescu was partially supported by a research fellowship of the University of Oulu, Finland, and by a grant of the Romanian National Authority for Scientific Research, CNCS-UEFISCDI, project PN-II-ID-PCE-2011-3-0709 (SOLACE). A.T. Aikio acknowledges Academy of Finland, grant number 285474. V. Pierrard thanks the Belgian Federal Scientific Policy Office for the interuniversity project P7/08 CHARM. The OMNI data were obtained from the GSFC/SPDF OMNIWeb interface at http://omniweb.gsfc.nasa.gov. The authors acknowledge the use of SuperDARN data. SuperDARN is a collection of radars funded by national scientific funding agencies of Australia, Canada, China, France, Italy, Japan, South Africa, United Kingdom and United States of America.

References

Anderson, P. C., R. A. Heelis, and W. B. Hanson (1991), The ionospheric signatures of rapid subauroral ion drifts, *J. Geophys. Res.*, *96*(A4), 5785–5792, doi:10.1029/90JA02651.

Anderson, P. C., D. L. Carpenter, K. Tsuruda, T. Mukai, and F. J. Rich (2001), Multisatellite observations of rapid subauroral ion drifts (SAID), *J. Geophys. Res.*, *106*(A12), 29,585–29,599, doi:10.1029/2001JA000128.

Anderson, P. C., W. R. Johnston, and J. Goldstein (2008), Observations of the ionospheric projection of the plasmapause, *Geophys. Res. Lett.*, *35*, L15110, doi:10.1029/2008GL033978.

Bandic, M., G. Verbanac, M. B. Moldwin, V. Pierrard, and G. Piredda (2016), MLT dependence in the relationship between plasmapause, solar wind and geomagnetic activity based on CRRES: 1990-1991, *J. Geophys. Res.*, 4397–4408, doi:10.1002/2015JA022278.

David, M., J. J. Sojka, R. W. Schunk, and R. Heelis (2002), Relative solar and auroral contribution to the polar *F* region: Implications for National Space Weather Program, *J. Geophys. Res.*, *107*, A101310, doi:10.1029/2001JA009167.

Deng, Y., and A. J. Ridley (2006), Dependence of neutral winds on convection *E*-field, solar EUV, and auroral particle precipitation at high latitudes, *J. Geophys. Res.*, *111*, A09306, doi:10.1029/2005JA011368.

Deng, Y., G. Lu, Y.-S. Kwak, E. Sutton, J. Forbes, and S. Solomon (2009), Reversed ionospheric convections during the November 2004 storm: Impact on the upper atmosphere, *J. Geophys. Res.*, *114*, A07313, doi:10.1029/2008JA013793.

Ebihara, Y., N. Nishitani, T. Kikuchi, T. Ogawa, K. Hosokawa, and M.-C. Fok (2008), Two-dimensional observations of overshielding during a magnetic storm by the Super Dual Auroral Radar Network (SuperDARN) Hokkaido radar, *J. Geophys. Res.*, *113*, A01213, doi:10.1029/2007JA012641.

Förster, M., S. Rentz, W. Köhler, H. Liu, and S. E. Haaland (2008), IMF dependence of high-latitude thermospheric wind pattern derived from CHAMP cross-track measurements, *Ann. Geophys.*, *26*, 1581–1595, doi:10.5194/angeo-26-1581-2008.

He, M., L. Liu, W. Wan, and B. Zhao (2011), A study on the nighttime midlatitude ionospheric trough, *J. Geophys., Res.*, *116*, A05315, doi:10.1029/2010JA016252.

Horvath, I., and E. A. Essex (2003), The Southern-Hemisphere mid-latitude day-time and night-time trough at low sunspot numbers, *J. Atmos. Sol. Terr. Phys.*, *65*, 917–940.

Lehtinen, M. S., and A. Huuskonen (1996), General incoherent scatter analysis and GUISDAP, *J. Atmos. Terr. Phys.*, *58*(1–4), 435–452, doi:10.1016/0021-9169(95)00047-x.

Mallis, M., and E. A Essex (1993), Diurnal and seasonal variability of the southern hemisphere main ionospheric trough from differential-phase measurements, *J. Atmos. Terr. Phys.*, *55*(7), 1021–1037.

Mendillo, M., J. Baumgardner, J. Wroten, C. Martinis, S. Smith, K.-D. Merenda, T. Fritz, M. Hairston, R. Heelis, and C. Barbieri (2013), Imaging magnetospheric boundaries at ionospheric heights, *J. Geophys. Res. Space Physics*, *118*, 7294–7305, doi:10.1002/2013JA019267.

Moffet, R. J., and S. Quegan (1983), The mid-latitude trough in the electron concentration of the ionospheric *F*-layer: A review of observations and modelling, *J. Atmos. Terr. Phys.*, *45*(5), 315–343.

Nilsson, H., T. I. Sergienko, Y. Ebihara, and M. Yamauchi (2005), Quiet-time mid-latitude trough: Influence of convection, field-aligned currents and proton precipitation, *Ann. Geophys.*, *23*, 3277–3288.

Nygrén, T., A. Aikio, R. Kuula, and M. Voiculescu (2011), Electric fields and neutral winds from monostatic incoherent scatter measurements by means of stochastic inversion, *J. Geophys. Res.*, *116*, A05305, doi:10.1029/2010JA016347.

Pavlov, A. V., and J. C. Foster (2001), Model/data comparison of *F* region ionospheric perturbation over Millstone Hill during the severe geomagnetic storm of July 15-16, 2000, *J. Geophys. Res.*, *106*, 29,051–29,069.

Pierrard, V., and J. Cabrera (2005), Comparisons between EUV/IMAGE observations and numerical simulations of the plasmapause formation, *Ann. Geophys.*, *23*(7), 2635–2646, SRef-ID: 1432-0576/ag/2005-23-2635.

Pierrard, V., and M. Voiculescu (2011), The 3D model of the plasmasphere coupled to the ionosphere, *Geophys. Res. Lett.*, *38*, L12104, doi:10.1029/ 2011GL047767.

Pryse, S. E., L. Kersley, M. J. Williams, and I. K. Walker (1998), The spatial structure of the dayside ionospheric trough, *Ann. Geophys.*, *16*, 1169–1179.

Redmon, R. J., W. K. Peterson, L. Andersson, and W. F. Denig (2012), A global comparison of O+ upward flows at 850 km and outflow rates at 6000 km during nonstorm times, *J. Geophys. Res.*, *117*, A04213, doi:10.1029/2011JA017390.

Rodger, A. S., R. J. Moffet, and S. Quegan (1992), The role of ion drift in the formation of ionization troughs in the mid- and high-latitude ionosphere—A review, *J. Atmos. Terr. Phys.*, *54*(1), 1–30.

Ruohoniemi, M., and R. A. Greenwald (1996), Statistical patterns of high-latitude convection obtained from Goose Bay HF radar observations, *J. Geophys. Res.*, *101*, 21,743–21,763.

Ruohoniemi, J. M., and K. B. Baker (1998), Large-scale imaging of high-latitude convection with Super Dual Auroral Radar Network HF radar observations, *J. Geophys. Res.*, *103*(A9), 20,797–20,811, doi:10.1029/98JA01288.

Schunk, R. W., P. M. Banks, and W. J. Raitt (1976), Effects of electric fields and other processes upon the nighttime high-latitude *F* layer, *J. Geophys. Res.*, *81*(19), 3271–3282, doi:10.1029/JA081i019p03271.

Schunk, R. W., and A. F. Nagy (1978), Electron temperature in the *F* region of the ionosphere: Theory and observations, *Rev. Geophys.*, *16*(3), 355–399.

Spiro, R. W., R. A. Heelis, and W. B. Hanson (1978), Ion convection and the formation of the mid-latitude *F* region ionization trough, *J. Geophys. Res.*, *83*(A9), 4255–4264, doi:10.1029/JA083iA09p04255.

Vanhamäki, H., A. Aikio, M. Voiculescu, L. Juusola, T. Nygrén, and R. Kuula (2016), Electrodynamic structure of the post-midnight high-latitude trough in summer, *J. Geophys. Res. Space Physics*, *121*, 2669–2682, doi:10.1002/2015JA022021.

Verbanac G., V. Pierrard, M. Bandic, F. Darrouzet, J.-L. Rauch, and P. Décréau (2015), Relationship between plasmapause, solar wind and geomagnetic activity between 2007 and 2011, *Ann. Geophys.*, *33*, 1271–1283.

Vlasov, M. N., and M. C. Kelley (2003), Modeling of the electron density depletion in the storm-time trough on April 20, 1985, *J. Atmos. Sol. Terr. Phys.*, *65*, 211–217.

Voiculescu, M., and T. Nygrén (2007), IMF effect on ionospheric trough occurrence at equinoxes, *Adv. Space Res.*, *40*, 1935–1940.

Voiculescu, M., and M. Roth (2008), Eastward sub-auroral ion drifts or ASAID, *Ann. Geophys.*, *26*, 1955–1963.

Voiculescu, M., I. Virtanen, and T. Nygrén (2006), The *F* region ionospheric trough: Seasonal dependence and relation to IMF, *24*, *1*, 173–185.

Voiculescu, M., T. Nygrén, A. Aikio, and R. Kuula (2010), An olden but golden EISCAT observation of a quiet-time ionospheric trough, *J. Geophys. Res.*, *115*, A10315, doi:10.1029/2010JA015557.

Werner, S., and G. W. Prölss (1997), The position of the ionospheric trough as a function of local time and magnetic activity, *Adv. Space Res.*, *20*(9), 1717–1722.

Whalen, J. A. (1989), The daytime *F* layer trough and its relation to ionospheric-magnetospheric convection, *J. Geophys. Res.*, *A12*, 17,169–17,184.

Zou, S., M. B. Moldwin, M. J. Nicolls, A. J. Ridley, A. J. Coster, E. Yizengaw, L. R. Lyons, and E. F. Donovan (2013), Electrodynamics of the high-latitude trough: Its relationship with convection flows and field-aligned currents, *J. Geophys. Res. Space Physics*, *118*, 2565–2572, doi:10.1002/jgra.50120.